

PCCP

Accepted Manuscript



This is an *Accepted Manuscript*, which has been through the Royal Society of Chemistry peer review process and has been accepted for publication.

Accepted Manuscripts are published online shortly after acceptance, before technical editing, formatting and proof reading. Using this free service, authors can make their results available to the community, in citable form, before we publish the edited article. We will replace this *Accepted Manuscript* with the edited and formatted *Advance Article* as soon as it is available.

You can find more information about *Accepted Manuscripts* in the [Information for Authors](#).

Please note that technical editing may introduce minor changes to the text and/or graphics, which may alter content. The journal's standard [Terms & Conditions](#) and the [Ethical guidelines](#) still apply. In no event shall the Royal Society of Chemistry be held responsible for any errors or omissions in this *Accepted Manuscript* or any consequences arising from the use of any information it contains.

Borazine: Spin Blocker? Or not?

Debojit Bhattacharya,^{a*} Suranjan Shil,^b Anirban Misra,^b Laimutis Bytautas^c
and Douglas J. Klein^a

^aDepartment of Marine Sciences, Texas A&M University at Galveston, Texas, 77553, USA

^bDepartment of Chemistry, University of North Bengal, Darjeeling, PIN. 734013, West Bengal, INDIA

^cGalveston College, Department of Chemistry, 4015 Avenue Q, Galveston, Texas, 77550, USA

*Telephone: (409) 740-4538, Email: debojitolora@gmail.com

Abstract

The spin blocker capacity of borazine is investigated. Specifically, *meta*-B-B, *meta*-N-N and *para*-B-N connected borazines are used as spin-blocker couplers comprised from a pair of radicals: two iminonitroxides (IN); IN and tetrathiafulvalene-radical-cation (TTF); or two TTFs. Density functional theory (DFT) is used to elucidate the spin blocker capacity of the linkage-specific (*meta* or *para*) borazine-coupler and elaborate the role of the lowest unoccupied molecular orbital (LUMO) in magnetic-exchange. Furthermore, a qualitative relation between different magnetic aromaticity indices is made using both nuclear-independent chemical shift (NICS) and the harmonic oscillator model of aromaticity (HOMA). The NICS values are calculated at the centre of the borazine spacer fragment of these diradical species and then also at 0.5 Å increments of the virtual probe from this centre position up to an orthogonal distance of 2.0 Å from the centre. The HOMA values are calculated for the borazine ring fragment in these diradicals. Based on the HOMA and NICS values, it is evident from that the borazine exhibits less aromatic character than benzene itself – due to the polar nature of B-N π -bonding. The LUMO mediated spin-exchange between the two consecutive singly occupied molecular orbitals (SOMOs) is explicitly discussed and confirmed to play a pivotal role. Parity of the coupler pathways, i.e. even or odd number of bonds along a selected pathway, between radical moieties is an important factor in predicting the nature and extent of magnetic exchange for these diradicals. Surprisingly, borazine does not always act as a spin-coupling blocker – rather in some cases the coupling is enhanced as compared to a homoatomic (carbon-based) benzene coupler.

Key Words: Borazine, Spin blocker coupler, Magnetic exchange, NICS, HOMA, HOMO, LUMO, SOMO, DFT.

1. Introduction

Next only to carbon, boron enjoys a richness in chemistry.¹⁻³ Boron-containing compounds have long fascinated chemists in some cases leading to exotic chemical-bonding patterns.⁴ A famous example is the diborane (B_2H_6) molecule where a B_2H_2 central fragment is being held together by two 3-center-2-electron bonds.⁵ The smallest elemental boron molecule is B_2 which had been a puzzling case for molecular spectroscopists for a very long time^[6]. Larger molecular structures made of elemental boron have been of high interest yielding a large variety of crystal structures. Although 3-D cage structures of boron dominate its chemistry, boron has received comparatively modest experimental attention^{7,8} as compared to its periodic neighbors. Substitution by boron and nitrogen in various cyclic conjugated hydrocarbons yield species applicable in pharmacology² and electronic materials.³ Meanwhile, other boron compounds have found application as reducing agents and temperature-resistant polymers in ceramics, catalysis and in other areas.⁹ Thus, there are numerous theoretical studies of B-N containing organic molecules^{10,11} often isoelectronic B-N pairs replacing C-C pairs, thereby giving a general class of structures that are similar to well-known conjugated hydrocarbons. The planarity and aromaticity versus antiaromaticity of boron clusters representing hydrocarbon-analogues have been investigated by Wang and co-workers.^{7,8} A theoretical analysis of comparatively ionic N-B-N- and B-N-B- substituted analogues of benzene have been made by Hoffmann and co-workers.¹² The degree of aromaticity in borazine has been a topic of some controversy¹³ starting soon after its discovery in 1926 by Stock and Pohland.¹⁴ The properties of borazine are in good agreement with a ring structure of six atoms which “on-the-average” represent a sp^2 hybridized-carbon. For the fully B-N substituted alternant species and polymers¹⁵ the simple Hückel-type model always gives a big HOMO-LUMO gap (of ≥ 4 eV), and a number of cages^{15b} of bucky-like shape have been studied theoretically. For graphene-related structures^{15c} where most of the carbons (but not all) are replaced by B and N atoms, a pattern has been elucidated that predicts a maximum number of carbon atoms replaced while maintaining a Hückel-type HOMO-LUMO gap of zero. However, a density-functional-theory (DFT) computation^[15c] gives a non-zero gap of ~ 0.1 eV, which in fact is very small compared to the

fully substituted species. Overall, the findings in ref. [15] suggest that while carbon and alternant BN molecules and tubes, share certain similarities between them they also can exhibit notable differences in their properties as well (depending on a specific case). The studies¹⁵ conclude that alternant BN molecules and tubes are stable and worthy of synthesis. Structural studies reveal that hexagonal (six-atom) BN-rings are planar with BN-bond-lengths that are close to bond-lengths of CC-bonds in benzene. Similarly, B-N-B bond-angles are comparable to C-C-C bond-angles in benzene. Recent computations by Hoffmann and coworkers¹² found that the C-C bond length of benzene is 1.390Å and for borazine the B-N bond length is 1.433Å. The authors in ref. [12] have suggested that the (B-N-B) systems deserve a greater degree of attention among researchers, thus providing a motivation for the present study.

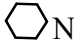
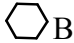
For the last few decades radicals, diradicals and polyradicals¹⁶ of organic origin have been widely studied due to their flexibility in applications in the field of magnetism,¹⁷ superconductivity,¹⁸ spintronics,¹⁹ photomagnetic behaviour²⁰ and others.²¹ In this study we choose iminonitroxides and tetrathiafulvalene-radical-cation as mono-radicals that are linked together by some coupler-species to yield diradical species. Iminonitroxide radicals are quite often chosen to study intramolecular spin-interactions.^{21f,22} Also, we note that while neutral tetrathiafulvalene (TTF) has unremarkable electrical properties, its cationic-species in fact exhibit semi-conducting properties (see, e.g. work by Ferraris *et al.* in ref. [23]). It is well known that in organic diradicals the character and the extent of magnetic interaction largely depends on the nature of a coupler between the two radical moieties.²¹ Spin densities on the spin-bearing atoms are excellent indicators of the nature and extent of exchange interactions.²⁴ There is evidence that bridges with delocalized π -electrons make a significant contribution to the nature of coupling between two radical moieties.²⁵ In the process of investigation of the intramolecular exchange-coupling constant (J) among various diradicals Koet *al.*²⁶ have found that J depends crucially on a length of the coupler. For example, a *meta*-phenylene fragment²⁷ has been found to be a robust and flexible organic high-spin coupler.

A qualitative prediction of the ground state of an open-shell radicaloid molecule is a challenging task and several methods have been developed to address this problem. Longuet-Higgins²⁸ introduced the first successful method for predicting ground-state multiplicities of radicaloid molecules. An alternative method was proposed by Ovchinnikov²⁹ and theoretically elucidated within the valence-bond (VB) formalism for planar alternant hydrocarbons by several

research groups.³⁰ These VB-based theoretic results are fully consonant^{30(b-c)} with the rule of spin-density alternation developed later in the context of the UHF treatment by Trindle *et al.*³¹ Heuristically, in planar π -conjugated system the spin densities of a particular atom prefer opposite signs to that of its adjacent neighbors, so that if the number of bonds is odd in the coupling path then the exchange is of antiferromagnetic nature. On the other hand, the net exchange coupling is of a high-spin form if the number of bonds in the coupling path between two π -conjugated magnetic sites is even. The VB theorems apply strictly to alternants (and rigorously) only to the homoatomic VB (or Heisenberg-spin) model. Thus, since here we have neither alternants nor homoatomic systems, the present study seeks to extend and generalize these ideas to enhance a physical insight on this subject.

The electronic structure of a molecule can be largely understood by examining its molecular orbitals. Among magnetic molecules the energy and shape of singly-occupied molecular orbitals (SOMOs) play an important role in predicting exchange interactions.^{21(a-c)} Using the extended Hückel theory, Hoffmann³² suggested that if the energy difference ($\Delta E_{SS} = E(SOMO)_1 - E(SOMO)_2$) is less than 1.5 eV, then a parallel orientation of spins occurs. Within the MO framework, one also needs to consider the differential overlap between the SOMOs, for which the arguments based on the Hund's rule are weakened if this differential overlap is very small (e.g., zero in the Hückel approximation).³³ The $4n$ - π antiaromatic linear and angular polyheteroacenes have been investigated by Constantinides and co-workers³⁴ using the B3LYP/6-31G(d,p) level of theory. The authors found³⁴ that if $\Delta E_{SS} > 1.3$ eV then a singlet ground-state with antiparallel orientation of spins results. However, Zhang *et al.*³⁵ have shown that a critical value of ΔE_{SS} depends on a system. Note, however that our systems are newly constructed so that the accurate values for ΔE_{SS} in these systems are not yet available in the literature. In general, the examination of SOMOs and their energies is not sufficient to elucidate the nature of magnetic interaction in organic molecules. We note that a spin-density alternation pattern between two radical moieties is a *critical* factor if the intervening coupler is alternant. Indeed, this is a consequence of a general model patterning in the overall antisymmetrical wavefunction as revealed in recent studies.³⁰

2. Selection of Diradicals

Here, we examine different diradicals coupled with borazine to study the effect of spin propagation through the coupler and elaborate the role of molecular orbitals, especially frontier orbitals. In particular, we seek to understand the spin exchange coupling which occurs through the conjugated π electron-system in a coupler. The exchange interactions are conventionally explained by the energy of SOMOs and their spatial distribution.²¹ Here, we discuss the intramolecular magnetic exchange of our constructed diradical systems in terms of their LUMOs, their SOMO₁-SOMO₂ as well as HOMO-LUMO energy gaps. Also, we shall analyze their molecular orbital spatial distribution as well as their spin-density fluctuations. The relative positions in 3-dimensional space of singly occupied orbitals, i.e. SOMO₁ and SOMO₂ as well as the LUMO play a significant role in the mechanism of exchange. In this work, we consider 10 diradical systems where *meta*- or *para*-connected borazine is used as a coupler. All 10 systems are divided into 3 groups, namely: the (IN)₂, the (IN-TTF) and the (TTF)₂ group, respectively. The proper structures of each of these 10 diradicals along with the atomic spin-populations up to three decimal places are depicted in **Scheme 3**. To understand these diradical species we look for the spin-density-alternation patterns through the borazine coupler. First of all, in the IN system the two sp³-carbons each have two C-H orbitals that couple to the IN π -network so that these C-H orbitals assume some slight spin-density opposite to each of the adjacent π -centers. On the other hand, the sp³-C spin-densities are parallel to one another in as much as the C-H bond orbitals on adjacent carbons, only couple weakly – below we shall not display these two (saturated) carbons in our π -network depictions. Secondly, in the IN system the spin-density on adjacent N and O is parallel, as is evidently due to an NO bond orbital for which the corresponding anti-bonding orbital is very high in energy. Consequently, this singly-occupied NO bonding orbital acts as a *single unified entity* with a single spin-density (the same on both N and O atoms). Thus, in later depictions we represent this NO bond orbital as a *single* (graphical) node. For each of these groups there are different modes of interconnection: *meta*-B-B-connected, *meta*-N-N-connected and *para*-B-N-connected borazines. Among these diradicals, (IN)₂ and (TTF)₂ groupings give just one *para*-connected species, while the IN-TTF grouping gives two *para*-B-N-connected diradicals, namely IN-B  N-TTF and IN-N  B-TTF). **Scheme 1S** of supporting information shows the atomic spin-populations up to two decimal places depicting only the π -network, neglecting the network which is purely σ , and the non-

alternant TTF moieties are represented as a single node. We forego *ortho*-connected species as these would certainly experience steric hindrance twisting the radical and the coupler π -planes to disrupt the π -electron network. This situation would be undesirable since our current aim is to investigate the itinerant exchange through an undisrupted but polarized π -network coupler (borazine).

3. Computational Methodology

Each of our studied structures is first optimized in the framework of density functional theory (DFT). Becke's three-parameter hybrid functional subsequently modified by Lee, Yang and Parr, *i.e.* B3LYP, along with 6-311G(d,p) Pople-type basis set is used for optimization via the Gaussian'09W³⁶ quantum chemical package. The choice of exchange-correlation functional is very important in DFT calculation. In the recent past, TTF, IN, nitronyl nitroxide (NN), verdazyl (V) based diradicals are widely studied using the well tested and popular B3LYP functional which was able to yield a reasonable agreement with the experimental magnetic exchange values in a numerous cases. Although different functionals may give different results for the same system, the B3LYP method, however is quite reliable in predicting exchange coupling constants for a varied range of organic diradicals.²¹ Following various previous studies¹⁷ the exchange coupling constants (J) of our designed diradicals are estimated by using the well-established and widely used Yamaguchi's broken-symmetry formula³⁷ within the DFT framework. This exchange constant is used with an effective Heisenberg spin Hamiltonian,

$$\hat{H} = -2J \hat{S}_1 \bullet \hat{S}_2, \quad (1)$$

where \hat{S}_1 and \hat{S}_2 are local spins on two components of radicals. The exchange-coupling parameter is given as:

$$J = \frac{(E_{BS} - E_T)}{(\langle S^2 \rangle_T - \langle S^2 \rangle_{BS})} \quad (2)$$

where, E_{BS} and E_T are energies of the broken-symmetry singlet (BS) and the triplet states, respectively. Here, $\langle S^2 \rangle_T$ and $\langle S^2 \rangle_{BS}$ are the corresponding average spin-square values.

Although the term aromaticity was introduced long ago, its conception in terms of reactivity, energetic, geometric and magnetic criteria has engendered an ambiguity in definition³⁸

as may be viewed to be due to a partially ordered^{38a-38b} or multidimensional^{38c} nature of aromaticity. This fact has led to various aromaticity quantifications, one of which is the harmonic oscillator model of aromaticity (HOMA)³⁹ – a geometrically based descriptor of aromaticity. The HOMA index³⁹ is one of the most reliable structural indices of local aromaticity. The HOMA index for each ring system can be evaluated via

$$HOMA = 1 - \frac{\alpha}{n} \sum_{i=1}^n (R_0 - R_i)^2 \quad (3)$$

where α is an empirical constant for a particular bond in a π system, n is the number of bonds taken in the summation, R_i is the calculated length of a specific bond in a given ring and R_0 is the optimal aromatic bond length taken from the literature. A HOMA value close to 1 indicates a high local aromaticity of the species. Here, we use standard values $\alpha = 72.03 \text{ \AA}^{-2}$ and $R_0 = 1.402 \text{ \AA}$ to calculate HOMA indices of the borazine ring fragment of the diradicals.^{39(d)}

The nucleus independent chemical shift (NICS) is another widely used magnetic aromaticity index, because of its efficacy via direct quantum chemical computation.⁴⁰ Both, HOMA and NICS can be used to classify aromaticity, non-aromaticity, and anti-aromaticity of a ring system. Note that although HOMA is often calculated globally (for a complete molecular structure) or locally (for a particular part of a molecule), we have evaluated just local HOMA values for the borazine ring fragment for each of the diradicals. The NICS magnetic aromaticity indices of borazine-rings as couplers in the diradical systems have been estimated using UB3LYP/GIAO methodology⁴⁰ with a 6-311G(d,p) basis set. First, we have calculated the NICS(0) values at the center of the borazine ring where the distance in z-axis direction (perpendicular to the ring) is zero, i.e. $R=0 \text{ \AA}$. Since the σ -framework of the C-C and C-H bonds affect the π -electron density of the aromatic ring additional NICS values, from NICS(0.5 \AA) to NICS(2 \AA) are calculated by placing the “virtual” probe neutron at regular increments of 0.5 \AA from the π -surface borazine ring of the coupler for each of these diradicals (see **Scheme 2**).

4. Results and Discussion

The *meta*-phenylene fragment is known as a proto-typical strong high-spin-favouring spacer between two spin-bearing sources.²⁷ In this work, however, we use linkage-specific couplers, 6 of which are *meta*-connected cyclic borazines and 4 of which are *para*-connected borazines. Such different linkage-specific borazine fragments serve as potential spin blockers

due to the higher electronegativity of N atoms in the borazine-ring fragment. Borazine sometimes is described as a π -aromatic compound.⁴¹ One would expect that the degree of aromaticity in borazine is lower than that of benzene since the degree of cyclic delocalization of electrons in the borazine ring should be reduced compared to that in benzene. Presumably, this is due to the large electronegativity difference between boron and nitrogen atoms in the former.

4.1. Aromaticity and Magnetism


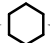
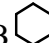
Aromaticity and magnetism are of fundamental importance in chemistry. However, unlike magnetism, aromaticity is of a multidimensional nature and can only be described within a partially ordered framework. In simple terms it means that the aromaticity cannot be described effectively only using a one-dimensional scale. The multidimensional character of aromaticity in heterocyclic compounds is advocated by Alonso and Herradón.⁴² Literature contains reports which describe the interrelation between aromaticity and magnetism in organic^{21c} and inorganic systems.⁴³ In general, aromaticity favors the ferromagnetic trend. It is noteworthy to mention that in open-shell systems the electron delocalization/aromaticity must be analyzed separately in each of the spin components, alpha and beta. That means that in some cases⁴⁴ radicals may display conflicting aromaticity (α versus β).

In general, one may expect that the magnetic-exchange coupling constant of a diradical depends on the aromaticity of the spin-coupler fragments.^{21b-21c} After its introduction in 1996, NICS has continually gained popularity as a useful aromaticity index.⁴⁰ Several authors⁴⁵ have pointed out, however, that NICS's validity to indicate diamagnetic ring currents is limited by the potential spurious contributions from the in-plane tensor components that are not related to aromaticity. This effect is partially avoided by using NICS(1) index that is considered to reflect more accurately the π -electron effects. Furthermore, its corresponding out-of-plane tensor component, NICS_{zz}(1), has been found to be useful in accurately describing π -electron effects.^{40d} In any event, one needs to keep in mind that NICS indices are based solely on theoretical considerations based on quantum theory, and unlike HOMA indices, cannot be determined by experimental means.

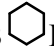
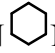
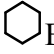
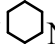
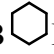
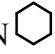
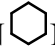
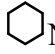
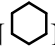
Table 2S (see supporting information) lists the NICS(X) values (in units of ppm) that have been calculated using GIAO/UB3LYP methodology. The NICS values for the coupler moieties are calculated after optimizing the corresponding diradical systems in their triplet state.

The trend of NICS(X) absolute values is: $\text{NICS}(0) < \text{NICS}(0.5\text{\AA}) < \text{NICS}(1\text{\AA}) > \text{NICS}(1.5\text{\AA}) > \text{NICS}(2\text{\AA})$ indicating the largest magnitude is observed for $X = 1\text{\AA}$. Furthermore, the zz -tensor component, i.e. $\text{NICS}_{zz}(1\text{\AA})$, has also been calculated for this height. **Table 1** displays the $\text{NICS}(1\text{\AA})$, $\text{NICS}_{zz}(1\text{\AA})$ and HOMA values, respectively. Note that the HOMA values have been calculated for all coupler fragments of the diradicals at their *triplet-multiplicity* optimized geometries. The plots in **Figure 1** compare the aromaticity indices with each other. Panel (A) displays the plot of HOMA versus $\text{NICS}_{zz}(1\text{\AA})$ and panel (B) displays the plot of HOMA versus $\text{NICS}(1\text{\AA})$ values. From the graphical display in **Figure 1** it is clear that HOMA and $\text{NICS}_{zz}(1\text{\AA})$ indices correlate much better with each other as compared to the HOMA versus $\text{NICS}(1\text{\AA})$. In general, HOMA indices are useful for describing electron delocalization effects in homonuclear systems, however, in case of heteroatoms⁴⁵ the usefulness of HOMA is less explored. On the other hand, NICS indices are considered to be more suitable for representing π -electron effects for heteroatomic systems. Thus, it is very satisfying to observe that HOMA and $\text{NICS}_{zz}(1\text{\AA})$ indices correlate rather well in our borazine-coupled diradicals.

From the data in **Table 1** it is evident that the magnitudes of $\text{NICS}(1\text{\AA})$ and $\text{NICS}_{zz}(1\text{\AA})$ values of the borazine ring fragment in these diradicals are much smaller compared to the ones in free benzene. One can argue that the low π -electron delocalization in borazine with respect to benzene is not only due to the electronegativity difference between N and B but also due to the polarized mesomeric structures that are present in borazine. In order to form and delocalize the π -N-B bonds, nitrogen atoms must support a positive charge whereas boron will have a negative charge. While these VB forms are possible, the weight in the total wave functions is expected to be small.

Next, we focus on the exchange coupling constants J to explore magnetic properties of our diradical systems. The relevant data is listed in **Table 2** where $J > 0$ values indicate ferromagnetically-coupled systems, and $J < 0$ values indicate anti-ferromagnetically-coupled systems. Finally, cases with $J = 0$ correspond to non-magnetic (diamagnetic) systems. In order to examine the correlation between the aromaticity indices, HOMA and $\text{NICS}_{zz}(1\text{\AA})$ and J values, in **Figure 2** we plot J versus HOMA, and in **Figure 3** we display J versus $\text{NICS}_{zz}(1\text{\AA})$ plots. It is clear that the best correlation is observed between exchange-coupling constants J and HOMA values *only* for ferromagnetically-coupled diradical systems with J values that are greater than 5 cm^{-1} . These systems are: IN-B  B-IN, IN-N  N-IN, and IN-B  N-TTF. For the remaining

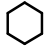
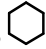
diradical systems the correlation between the aromaticity indices (HOMA and NICS) and J values is not transparent.

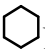

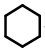
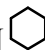
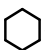
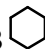
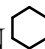
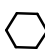

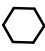
If we compare the HOMA values of (IN)₂ borazine-coupled systems, we find that the HOMA value of diradical IN-B  B-IN is higher than in the diradical IN-N  N-IN. In addition, it is clear that IN-B  B-IN ($J=41.70 \text{ cm}^{-1}$) displays a stronger ferromagnetic coupling than the IN-N  N-IN system ($J=21.94 \text{ cm}^{-1}$). The comparison of *all* our *meta*-connected diradicals implies that the B-B-*meta* species generally exhibit larger HOMA values than the corresponding N-N-*meta* diradicals. For example, if we take the *low-spin meta*-structures (meta-B-B and meta-N-N), i.e. IN-B  B-TTF and IN-N  N-TTF, one observes that NN-connected structure (HOMA=0.869) exhibits a more pronounced *antiferromagnetic* coupling than BB-connected structure (HOMA=0.946). This seems to imply that N-N-connected-species tend favor *more negative* J values compared to the B-B-connected *meta*-connected diradicals. This observation seems to suggest that more electronegative atoms, when used as connectors between monoradical species, tend to result structures with lower HOMA and more negative J values. The lowest HOMA values are observed for IN-N  N-TTF, IN-B  N-TTF, and TTF-N  N-TTF diradicals. A notable feature in these structures is that the connecting atoms that link monoradical moieties to the borazine coupler contain N-atoms. In fact, both the *meta*-structures have the NN-connection, and only the *para*-structure has the BN-connection.

Recalling that for the singlet-state one has $\langle S^2 \rangle = 0$ and for the triplet-state one has $\langle S^2 \rangle = 2$ we can discuss the spin-states of our diradical systems in more detail. We see that the $\langle S^2 \rangle$ values for the UHF triplets are uniformly near $1(1+1) = 2$, while for the UHF broken-symmetry states, $\langle S^2 \rangle$ values are approximately half-way between triplet and singlet, i.e. close to 1. Thus, the computed J values evidently are reasonable. The data in **Table 2** indicates that four diradicals are high-spin, one is diamagnetic (has uncoupled mono-radicals with $J = 0$) and the remaining five are low-spin. The table indicates that the (IN)₂ group has two high-spin and one low-spin species, whereas in the (IN-TTF) group one finds one high-spin and three low-spin diradicals. In the (TTF)₂ group we find one each of high-spin, low-spin and diamagnetic diradicals. **Table 2** further reveals that the *meta*-connected diradicals are high-spin for groups (IN)₂ and (TTF)₂ with

an exception for diradical TTF-NC1=CC=CC=C1N-TTF which is diamagnetic. On the other hand, the *meta*-connected diradicals for (IN-TTF) group are low-spin. Between two *para*-connected diradicals of the (IN-TTF) group we find a change of sign of the exchange-coupling constant as the connecting atoms with the radical moieties in the borazine coupler are interchanged (N/B or B/N), i.e. structures **5** and **6**. Much of this is rationalized in the next subsection with the spin-density alternation rule as in ref. [24(b,c)], here applied in an extended hetero-atom context. For the (TTF)₂ group diradical series, the aromaticity indices NICS_{zz}(1Å) and HOMA indicate that the structure TTF-BC1=CC=CC=C1B-TTF ($J = 2.20 \text{ cm}^{-1}$) is more aromatic than the structure TTF-NC1=CC=CC=C1N-TTF which is actually diamagnetic ($J = 0$), evidently indicating a lack of itinerant exchange albeit with π -electron dispersion in the coupler moiety.

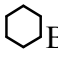
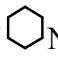
As can be seen from the data in **Table 3**, the parity of spin propagation pathway correctly predicts the sign of the J exchange coupling constant in 8 out of 10 diradicals which is very encouraging. Recall that *even* number of bonds along the spin propagation pathway are predicted to yield high-spin ($J > 0$) states and *odd* number of bonds along such pathway are expected to yield low-spin ($J < 0$) ground states. The *only* exceptions are IN-NC1=CC=CC=C1B-TTF and TTF-NC1=CC=CC=C1N-TTF. Clearly, the exchange coupling for the species IN-NC1=CC=CC=C1B-TTF is out of line with our expectations compared to IN-BC1=CC=CC=C1N-TTF – indeed the sign of exchange-coupling constant J is opposite to what is expected. The expectation that the sign of J correlates with the parity of the length of the π -network pathway between radical moieties is followed in most of our other calculations where the values of $\langle S^2 \rangle$ for the triplet and broken-symmetry (BS) states tend to support the presumptions in Yamaguchi's formula³⁷ for J . The correlation of the length-parity with the sign of exchange-coupling constant is consistent with spin-density alteration pattern observed in the data of **Scheme 3**. A suggestion of the discrepancy in the case of IN-NC1=CC=CC=C1B-TTF is also found in the difference between J values calculated using B3LYP and M06 functionals (see **Table 2**). For example, while the J values calculated using B3LYP and M06 functionals for the IN-BC1=CC=CC=C1N-TTF system are 8.78 cm^{-1} and 2.19 cm^{-1} , respectively, for the IN-NC1=CC=CC=C1B-TTF system, the J values are -132.89 cm^{-1} and -12.78 cm^{-1} , respectively. Clearly, the calculated J value is much more sensitive to the type of DFT functional in the case of the IN-N

B-TTF system as compared to IN-BN-TTF. Our choice of selecting the M06 functional was based on literature reports indicating that M06 functional has been successful⁴⁶ for predicting the magnetic exchange coupling constants in organic and inorganic open-shell molecules^{46(a)} along with other physical properties in metal complexes also.^{46(b)}

From the J values of benzene bridged diradicals we find that m -benzene coupled (having carbon atom with intermediate electronegativity) diradicals have always intermediate J values than that of the m -BB (having lower electronegativity) and m -NN (having higher electronegativity) connected borazine bridged diradicals irrespective of the radical moieties. Note that the atomic spin-population in connecting N atoms of the borazine coupler is zero (**Scheme 3**) for diradical TTF-NN-TTF, and hence the species should exhibit diamagnetic behavior. The related TTF-BB-TTF species also have nearly zero spin-densities though larger in 3rd-decimal place, and ends up being just very slightly ferromagnetically-signed. For the diradical IN-NN-TTF the atomic spin-population does not follow the regular change of sign, although these anomalous non-alternating spin-densities are essentially zero. In the case of diradical IN-NN-IN the atomic spin-population values at the connecting N atoms of the borazine coupler are much smaller compared of the atomic spin-populations in the corresponding B atoms in the diradical IN-BB-IN. **Figure 4** shows the regular spin-density alternation plots of these diradicals. It is evident that the *high-spin* diradicals, (i.e. IN-BB-IN, IN-NN-IN, IN-BN-TTF, TTF-BB-TTF) display the *regular* spin-density alternation. On the other hand, in the rest of the systems the spin-propagation is effectively blocked through the coupler, as might be expected as they are “low-spin”. In the N-O bond of the IN moiety the unpaired electron resides solely in the bonding MO (see the net spin population of N and O atoms for the N-O group in **Figure 4**). The species IN-NB-TTF with an anomalous J value is also seen to manifest an anomalous (near-zero) spin alternation pattern through the coupler.

The comparison of these J values with the other diradicals where m - and p -phenylenes are used as couplers is of interest. In general, m - and p -phenylene couplers produce high-spin and low-spin ground states, respectively when they are attached to two radical moieties.²¹

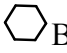
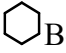
However, depending upon the planarity of the molecule, length (parity) of the coupling pathway, presence of heteroatoms, *m*- and *p*-phenylenes can also act as low-spin^{41,47} and high-spin^{21(d)} couplers, respectively. Depending upon the twisting angle, *m*-phenylene bridged-compounds can yield large exchange coupling constants through heterocyclic couplers.^{21(d)} The observations above can be explained in light of spin-density alternation plots via Mulliken atomic-spin populations through the coupler fragment. As mentioned above, we see that the *meta*-N-N-connected diradicals show lower values of J compared to their corresponding *meta*-B-B-connected diradicals.

An overall graphical representation exhibiting the effect on the magnetic properties of diradical systems produced by the substitution of the borazine-coupler in place of the benzene-ring is displayed in **Figure 5**. Here, we plot J values for two cases: (a) when borazine as a coupler (blue symbols) or benzene as a coupler (red symbols) for all 10 diradical systems. The J values are plotted versus the label of a diradical system following the numbering convention of **Table 1**. The high-spin states correspond to cases where $J > 0 \text{ cm}^{-1}$ and low-spin systems are represented by $J < 0 \text{ cm}^{-1}$ values. Finally, the diradical states with $J = 0 \text{ cm}^{-1}$ values correspond to diamagnetic (non-magnetic) states. It is evident that in a few cases blue symbols are actually above the red ones, meaning that in some cases borazine-ring is actually able to *enhance* the high-spin (ferromagnetic) character of diradicals, like, for example, in the IN-B  B-IN system. In other cases, however, the situation is reversed, for instance in the IN-N  N-IN system where the borazine-ring acts as a *spin blocker* reducing the ferromagnetic character of the ground state.

Further information is displayed in **Scheme 4** which shows the atomic spin-population for the corresponding benzene-coupled diradicals with the same radical moieties as in borazine coupler. By comparing **Schemes 3** and **4** it is evident that in the borazine-coupled diradicals the total atomic spin-population of coupler borazine moieties varies from 0.00 to 0.05 depending on the nature of the bonding. On the other hand, in the benzene-bridged diradicals the total atomic spin-population in the benzene coupler varies from 0.09 to 0.20. Thus, the variation of the total atomic spin-population is much more significant in benzene as compared to the corresponding borazine coupler. Moreover, for the benzene coupler a strong regular change of sign of atomic-spin is observed regardless of the type of radical moieties, whereas, for the borazine coupler this type of regular atomic spin-population is often suppressed to near-zero values.

4.3. The Role of SOMOs and LUMO in Magnetic Interaction

In the studies of magnetism, the spatial distribution of the molecular orbitals (MOs) is an important factor.^{21(a,d)} The spatial distribution of the two magnetic (singly-occupied SOMO-1 and SOMO-2) and virtual MOs for each of these diradicals is represented in **Figure 6**. In our previous investigations,^{21(a,c)} it was found that the disjoint magnetic orbitals can explain the nature of magnetic interaction. In **Figure 6** one can see that the spatial distribution of the SOMOs is located on separate monoradical moieties. Generally, the molecule can easily undergo itinerant exchange between two unpaired spins situated in two different SOMOs through the vacant LUMO. In spin-polarized calculation, spin-up (α) and spin-down (β) electrons occupy different molecular orbitals. In fact, molecular magnetism arises due to the interaction of two unpaired electrons residing in SOMO-1 and SOMO-2 (in **Figure 6** they are labeled as HOMO-1 and HOMO). Clearly, these two orbitals exhibit a localized character. In **Figure 6** we also display LUMO and LUMO+1 orbitals, as they can participate in the spin exchange-coupling mechanism as discussed above. For (IN)₂ diradicals the three major MOs indicated above *fully cover* the respective diradicals. Thus, the itinerant exchange between the two unpaired spins (SOMOs) through the coupler can be facilitated.

Table 4 lists the SOMO-SOMO and HOMO-LUMO energy gaps for each of the molecules in this study. Diradicals IN-N  B-TTF and TTF-B  B-TTF possess the largest and the smallest SOMO-SOMO energy gaps, respectively. It is of interest to explore the correlation between structural symmetry properties and their SOMO-1 and SOMO-2 energy gaps, i.e. $\Delta E_{\text{SOMO-SOMO}}$. The relevant data is displayed in **Table 5**. Two structural symmetry indicators are considered in this context. The first is based on monoradical-pairs, and the second is based on connector-atoms. The symmetric (SYM) monoradical combinations are: (IN,IN), (TTF,TTF) and non-symmetric (NONSYM) monodiradical combination is (IN,TTF). The symmetric (SYM) connector-atom combinations are: (B,B) and (N,N) while the non-symmetric (NONSYM) connector-atom combination is (B,N). It is reasonable to expect that if mono-radical species on both sides of the coupler-ring are *identical* (i.e. SYM), then SOMO-1 and SOMO-2 orbital energies (where SOMO-1 is localized on one of the mono-radical species and SOMO-2 is localized on another mono-radical center located on the opposite side from the coupler) should be very close to each other. This means that $\Delta E_{\text{SOMO-SOMO}}$ should be very small. On the other hand, if the mono-radical moieties represent different species, then one would expect the

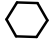
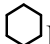
$\Delta E_{\text{SOMO-SOMO}}$ value to be fairly large. This is exactly what is observed in **Table 5**. The four systems (structures **4** to **7**) exhibiting large SOMO-SOMO gaps are listed in bold and represent NONSYM-combination for monoradical pairs. Thus, the calculated values are manifestly reasonable and accurately reflect the variations in molecular environment. The connector-atom effect is of only a minor importance, although the NONSYM/NONSYM combination in the structure IN-N  B-TTF corresponds to the largest SOMO-SOMO gap as expected. The high-spin diradical IN-B  B-IN has the smallest SOMO-SOMO energy gap (except for the diamagnetic species) with the *highest value* of high-spin exchange constant J . A graphical representation of the correlation between the HOMO-LUMO and SOMO-SOMO gaps is depicted in **Figure 7** reflecting a strong degree of correlation.

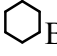
Table 6 lists natural orbital occupations of different orbitals calculated using spin-polarized DFT at UB3LYP/6-311(d,p) level.^{44,50} It is evident that in all of the magnetic orbitals the occupation is 1, the HOMO-2 has occupation just below 2, while the LUMO has small natural orbital occupation numbers. This means that the LUMO takes part in the itinerant exchange mechanism between the unpaired spins through the spacer. The last three diradicals exhibit coupling constants J of small magnitude and also the lowest LUMO occupations. Therefore, we can argue that the magnitude of LUMO occupation number somewhat correlates with the magnitude of J in these systems. However, a close correlation between the values of LUMO and exchange coupling constants for all 10 diradical systems cannot be established from the available data.

5. Conclusions

We have examined ten related diradicals for which *meta*- and *para*-connected BN-heteroatomic borazine ring fragments are used as couplers. Among these diradicals there are three types, where (IN)₂, (TTF)₂ and IN-TTF groupings are taken with our π -spacers *viz.* *meta*-B-B-, *meta*-N-N-, and *para*-B-N-borazine moieties. We seek to understand the magnetic properties of BN-alternant heterocyclic π -electron systems and how they relate to the aromaticity criteria. We have studied the ability of borazine as spin blocker by analyzing all possible combinations of two radical moieties (IN and TTF) connected through the borazine coupler. Correlation between the aromaticity and spin-density polarization in borazine is established using magnetic and

geometric criteria. The effect of the spin propagation through the borazine coupler has been assessed using aromaticity descriptors, exchange-coupling constants, spin-density distributions and atomic spin-populations. In addition, the role of the frontier molecular orbitals in the magnetic exchange is discussed. We used the HOMA index to gain a qualitative understanding of the relationship between the aromaticity and magnetic properties. As expected, both aromaticity indices (NICS and HOMA) reveal that borazine is less aromatic than benzene. Although with the use of TTF as radical moieties, many researchers have observed high J values between TTF radical moieties, for our couplers we find small J values. The best correlation has been observed between J and HOMA values for ferromagnetic (high-spin) systems with $J > 5$ cm⁻¹. Also, a reasonable correlation has been found between HOMA and NICS_{zz}(1Å) values for all 10 systems.

From the spin-density alternation plots it is evident that for the high-spin diradicals the regular spin-density alternation occurs whereas for the low-spin species the alternation of spin-density is more effectively blocked through the coupler. This correlates with the fact that the B-N bonds are somewhat polar with the π -electrons more localized at the more electronegative N atoms. The mechanism of itinerant exchange is explained by the spatial distribution of the LUMO. Usually, a spin-alternation pattern persists through the borazine coupler, although the degree is notably reduced compared to the benzene coupler. The knowledge of the spin alternation pattern enables a robust prediction of ferro- vs. antiferro-magnetic signs for the exchange-coupling constant J . Furthermore, the parity of spin propagation pathway provides an effective tool for predicting the sign of the exchange coupling constant J in the challenging case of heteroatomic systems. In fact, the parity consideration yields a correct prediction for 8 out of 10 borazine-coupled diradicals which is highly satisfactory keeping in mind that, in contrast to the heteroatomic systems, so far only for homoatomic (carbon-based) bipartite structures the accurate rules regarding ground-state multiplicities are available.⁵¹

Surprisingly, depending on the molecular environment and how the mono-radical species are linked together via a coupler, the borazine molecule can act as a spin-blocker (compared to benzene) in some cases. In other cases, the use of borazine molecule instead of benzene greatly enhances the magnetic exchange coupling, like in the case of IN-B  B-IN. Overall, this work provides a novel insight concerning the effects of heteroatomic structures in the spin coupling of radicals via conjugated π -network systems.

Supporting Information

The optimized XYZ co-ordinates with respective optimized geometries, complete reference 30, atomic spin-populations up to two decimal points for the whole molecules depicting only the π -network, neglecting the network which is purely σ , and the non-alternant TTF moieties are represented as a single node, spin-density alternation plots and J values of **Scheme 4** molecules.

Acknowledgements

DB and DJK acknowledge the support (via grant BD-0894) of the Welch Foundation of Houston, Texas. AM and SS thank CSIR, India for financial support. DB specially thanks Tamal Goswami for his support in addressing the reviewers' comments.

References:

- [1] M. J. D. Bosdet, W. E. Piers, *Can. J. Chem.* **2009**, *87*, 8.
- [2] (a) C. W. Levy, C. Baldock, A. J. Wallace, S. Sedelnikova, R. C. Viner, J. M. Clough, A. R. Stuitje, A. R. Slabas, D. W. Rice, J. W. Rafferty, *J. Mol. Biol.* **2001**, *309*, 171.
(b) M. A. Grassberger, F. Turnowsky, J. Hildebrandt, *J. Med. Chem.* **1984**, *27*, 947.
- [3] Y. Lu, A. Bolag, J. Nishida, Y. Yamashita, *Synth. Met.* **2010**, *160*, 1884.
- [4] A. N. Alexandrova, A. I. Boldyrev, H.-J. Zhai, L.-S. Wang, *Coordination Chemistry Reviews*, **2006**, *250*, 2811.
- [5] W. H. Eberhardt, B. Jr. Crawford, W. N. Lipscomb, *J. Chem. Phys.* **1954**, *22*, 989.
- [6] L. Bytautas, N. Matsunaga, G. E. Scuseria, K. Ruedenberg, *J. Phys. Chem. A* **2012**, *116*, 1717.
- [7] H. Zhai, B. Kiran, J. Li, L. Wang, *Nature Materials*, Hydrocarbon Analogues of Boron Clusters - Planarity, Aromaticity and Antiaromaticity. **2003**, *2*, 827.
- [8] H.-J. Zhai, Y.-F. Zhao, W.-L. Li, Q. Chen, H. Bai, H.-S. Hu, Z. A. Piazza, W.-J. Tian, H.-G. Lu, Y.-B. Wu, Y.-W. Mu, G.-F. Wei, Z.-P. Liu, J. Li, S.-D. Li, L.-S. Wang, *Nature Chemistry*, **2014**, *6*, 727.
- [9] J. Casanova, *The Borane, Carborane, Carbocation Continuum*, New York, John Wiley and Sons, Inc. 1998.
- [10] M. J. S. Dewar, R. C. Dougherty, *J. Am. Chem. Soc.* **1964**, *86*, 433.

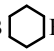
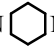
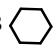
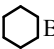
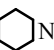
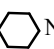
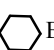
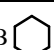

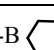
- [11] E. L. Muetterties, *The Chemistry of Boron and Its Compounds*; Wiley: New York, 1967.
- [12] K. AlKaabi, P. L. V. K. Dasari, R. Hoffmann, *J. Am. Chem. Soc.* **2012**, *134*, 12252.
- [13] Islas, R.; Chamorro, E.; Robles, J.; Heine, T.; Santos, J. C.; Merino, G. *Struct. Chem.* **2007**, *18*, 833.
- [14] A. Stock, E. Pohland, *Chem. Ber.* **1926**, *59B*, 2215 and references therein.
- [15] (a) H.-Y. Zhu, D. J. Klein, W. A. Seitz, and N. H. March, *Inorg. Chem.* **1995**, *34*, 1377.
(b) H.-Y. Zhu, T. G. Schmalz, D. J. Klein, *Int. J. Quantum Chem.* **1997**, *63*, 393.
(c) H.-Y. Zhu, D. J. Klein, N. H. March, *J. Phys. Chem. Solids* **1998**, *59*, 1303.
- [16] O. Kahn, *Molecular Magnetism*; VCH: New York, 1993.
- [17] P. M. Lahti, *Magnetic Properties of Organic Materials*; Marcel Dekker: New York, 1999.
- [18] S. Uji, H. Shinagawa, T. Terashima, T. Yakabe, Y. Terai, M. Tokumoto, A. Kobayashi, H. Tanaka, H. Kobayashi, *Nature* **2001**, *410*, 908.
- [19] G. A. Prinz, *Science* **1998**, *282*, 1660.
- [20] N. Tanifuji, M. Irie, K. Matsuda, *J. Am. Chem. Soc.* **2005**, *127*, 13344.
- [21] (a) D. Bhattacharya, A. Misra, *J. Phys. Chem. A* **2009**, *113*, 5470.
(b) D. Bhattacharya, S. Shil, A. Misra, D. J. Klein, *Theor. Chem. Acc.* **2010**, *127*, 57.
(c) D. Bhattacharya, S. Shil, A. Panda, A. Misra, *J. Phys. Chem. A* **2010**, *114*, 11833.
(d) V. Polo, A. Alberola, J. Andres, J. Anthony, M. Pilkington, *Phys. Chem. Chem. Phys.* **2008**, *10*, 857.
(e) D. Bhattacharya, S. Shil, A. Misra, *J. Photochem. Photobios. A Chem.* **2011**, *217*, 402.
(f) D. Bhattacharya, A. Panda, S. Shil, T. Goswami, A. Misra, *Phys. Chem. Chem. Phys.* **2012**, *14*, 6905.
(g) D. Bhattacharya, S. Shil, T. Goswami, A. Misra, A. Panda, D. J. Klein, *Comp. Theo. Chem.* **2013**, *1024*, 15.
(h) D. Bhattacharya, S. Shil, T. Goswami, A. Misra, D. J. Klein, *Comp. Theo. Chem.* **2014**, *1039*, 11.
(i) Md. E. Ali, P. M. Oppeneer, *J. Phys. Chem. Lett.* **2011**, *2*, 939.
(j) M. Podewitz, C. Herrmann, A. Malassa, M. Westerhausen, M. Reiher, *Chem. Phys. Lett.* **2008**, *451*, 301.
(k) C. Herrmann, M. Podewitz, M. Reiher, *Int. J. Quantum Chem.* **2009**, *109*, 2430.

- (l) B. N. Papas, S. Wang, N. J. DeYonker, H. L. Woodcock, H. F. Schaefer, *J. Phys. Chem. A* **2003**, *107*, 6311.
- [22] J. Akita, K. Kobayashi, *Tetrahedron*, **1996**, *52*, 6893.
- [23] J. Ferraris, D. O. Cowan, V. V., Jr. Walatka, J. H. Perlstein, *J. Am. Chem. Soc.* **1973**, *95*, 948.
- [24] K. C. Ko, D. Cho, J. Y. Lee, *J. Phys. Chem. A* **2012**, *116*, 6837.
- [25] V. Barone, I. Cacelli, A. Ferretti, *J. Chem. Phys.* **2009**, *130*, 094306.
- [26] K. C. Ko, D. Cho, J. Y. Lee, *J. Phys. Chem. A* **2013**, *117*, 3561.
- [27] (a) A. Rajca, *J. Am. Chem.Soc.* **1990**, *112*, 5890.
(b) K. Itoh, *Pure Appl. Chem.* **1978**, *50*, 1251.
- [28] H. C. Longuet-Higgins, *J. Chem. Phys.* **1950**, *18*, 265.
- [29] A. A. Ovchinnikov, *Theor.Chim.Acta* **1978**, *47*, 297.
- [30] (a) D. J. Klein, C. Nelin, S. Alexander, F. A. Matsen, *J. Chem. Phys.* **1982**, *77*, 3101.
(b) A. A. Ovchinnikov, V. O. Cheranovskii, *Theor.Exptl Chem.* **1980**, *16*, 119 (English translation).
- (c) D. J. Klein, S. A. Alexander, Organic Polyradicals, High-Spin Hydrocarbons, and Organic Ferromagnets, Chemical Applications of Topology and Graph Theory. ed.R. B. King (Elsevier Pub., Amsterdam, 1987, pp 404-419).
- [31] (a) C. Trindle, S. N. Datta, *Int. J. Quantum Chem.* **1996**, *57*, 781.
(b) C. Trindle, S. N. Datta, B. Mallik, *J. Am. Chem. Soc.* **1997**, *119*, 12947.
- [32] R. Hoffmann, G. D. Zeiss, G. W. Van Dine, *J. Am. Chem. Soc.* **1968**, *90*, 1485.
- [33] W. T. Borden, E. R. Davidson, *Acc. Chem. Res.* **1981**, *14*, 69.
- [34] C. P. Constantinides, P. A. Koutentis, J. Schatz, *J. Am. Chem. Soc.* **2004**, *126*, 16232.
- [35] G. Zhang, S. Li, Y. Jiang, *J. Phys. Chem. A* **2003**, *107*, 5573.
- [36] M. J. Frisch, G. W. Trucks, H. B. Schlegel, G. E. Scuseria, M. A. Robb, J. R. Cheeseman, G. Scalmani, V. Barone, B. Mennucci, G. A. Petersson, *et al.* Gaussian 09, revision B.01; Gaussian, Inc.: Wallingford, CT, 2010.
- [37] (a) K. Yamaguchi, Y. Takahara, T. Fueno, K. Nasu, *Jpn. J. Appl. Phys.* **1987**, *26*, L1362.
(b) K. Yamaguchi, F. Jensen, A. Dorigo, K. N. Houk, *Chem. Phys.Lett.* **1988**, *149*, 537.
- [38] (a) D. J. Klein, *J. Chem. Ed.* **1992**, *69*, 691.
(b) D. J. Klein, D. Babić, *J. Chem. Inf. Comp. Sci.* **1997**, *37*, 656.

- (c) A. Katritzky, P. Barczynski, G. Musumarra, D. Pisano, M. Szafran, *J. Am. Chem. Soc.* **1989**, *111*, 7.
- [39] (a) J. Kruszewski, T. M. Krygowski, *Tetrahedron Lett.* **1972**, 3839.
- (b) T. M. Krygowski, A. Ciesielski, C. W. Bird, A. Kotschy, *J. Chem. Inf. Comput. Sci.* **1995**, *35*, 203.
- (c) T. M. Krygowski, M. Cyrański, A. Ciesielski, B. Świrski, P. Leszczyński, *J. Chem. Inf. Comput. Sci.* **1996**, *36*, 1135.
- (d) I. D. Madura, T. M. Krygowski, M. K. Cyrański, *Tetrahedron* **1998**, *54*, 14913.
- (e) T. M. Krygowski, J. E. Zachara, H. Szatylwicz, *J. Org. Chem.* **2004**, *69*, 7038.
- (f) T. M. Krygowski, M. K. Cyrański, *Chem. Rev.* **2001**, *101*, 1385.
- [40] (a) Z. Chen, C. S. Wannere, C. Corminboeuf, R. Puchta, P. v. R. Schleyer, *Chem. Rev.* **2005**, *105*, 3842.
- (b) P. v. R. Schleyer, M. Manoharan, H. Jiao, F. Stahl, *Org. Lett.* **2001**, *3*, 3643.
- (c) P. v. R. Schleyer, C. Maerker, A. Dransfeld, H. Jiao, N. J. R. v. E. Hommes, *J. Am. Chem. Soc.* **1996**, *118*, 6317.
- (d) H. Fallah-Bagher-Shaidaei, C. S. Wannere, C. Clorminboeuf, R. Puchta, P. v R. Schleyer, *Org. Lett.* **2006**, *8*, 863.
- [41] B. Kiran, *Inorg. Chem.* **2001**, *40*, 3615.
- [42] M. Alonso, B. Herradón, *Phys. Chem. Chem. Phys.* **2010**, *12*, 1305.
- [43] (a) S. Paul, A. Misra, *Inorg. Chem.* **2011**, *50*, 3234.
- (b) S. Paul, T. Goswami, A. Misra, P. K. Chattaraj, *Theor. Chem. Acc.* **2013**, *132*, 1391.
- [44] (a) M. Mandado, A. M. Graña, I. Pérez-Juste, *J. Chem. Phys.* **2008**, *129*, 164114.
- (b) A. Soncini, P. W. Fowler, *Chem. Eur. J.* **2013**, *19*, 1740.
- [45] (a) T. M. Krygowski, M. K. Cyrański, *Phys. Chem. Chem. Phys.* **2004**, *6*, 249.
- (b) A. Stanger, *Chem. Commun.* **2009**, 1939.
- (c) P. Seal, S. Chakrabarti, *J. Phys. Chem. A* **2007**, *111*, 9988.
- [46] (a) R. Valero, R. Costa, I. de P. R. Moreira, D. G. Truhlar, F. Illas, *J. Chem. Phys.* **2008**, *128*, 114103.
- (b) D. Bhattacharya, S. Shil, S. Sarkar, A. Misra, *J. Phys. Chem. A* **2013**, *117*, 4945.
- [47] (a) M. Dvolaitzky, R. Chiarelli, A. Rassat, *Angew. Chem. Int. Ed. Engl.* **1992**, *31*, 180.
- (b) F. Kanno, K. Inoue, N. Koga, H. Iwamura, *J. Am. Chem. Soc.* **1993**, *115*, 847.

- [48] S. Fang, M. Lee, D. A. Hrovat, W. T. Borden, *J. Am. Chem. Soc.* **1995**, *117*, 6727.
- [49] (a) L. Serrano-Andres, D. J. Klein, P. v. R. Schleyer, J. M. Oliva, *J. Chem. Theo. Comp.* **2008**, *4*, 1338.
- (b) J. M. Oliva, L. Serrano-Andres, D. J. Klein, P. v. R. Schleyer, J. Michl, *Intl. J. Photoenergy* **2009**, *2009*, 292393(1).
- (c) J. M. Oliva, L. Serrano-Andrés, *J. Comp. Chem.* **2005**, *27*, 524.
- (d) J. M. Oliva, D. J. Klein, P. v. R. Schleyer, L. Serrano-Andrés, *Pure Applied Chem.* **2008**, *81*, 719.
- (e) J. M. Oliva, D. R. Alcoba, L. Lain, A. Torre, *Theo. Chem. Acc.* **2013**, *132*, 1329(1).
- (f) J. M. Oliva, L. Serrano-Andrés, Z. Havlas, J. Michl, *J. Mol. Struct.– THEOCHEM*, **2009**, *912*, 13.
- [50] Y. Takano, K. Yamaguchi, and H. Nakamura, Chemical Indices of the Biomimetic Models of Oxyhemocyanin and Oxytyrosinase, *Biomimetic Based Applications*, Prof. Marko Cavrak (Ed.), **2011**, chapter 8, 183-200 pp.; ISBN: 978-953-307-195-4, InTech-publishers.
- [51] D. J. Klein, L. Bytautas, *J. Phys. Chem. A* **1999**, *103*, 5196.

Table 1. Calculated NICS^a and HOMA^b values for the linkage-specific borazine moieties at the UB3LYP level using a 6-311G(d, p) basis set for each diradical.

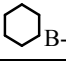
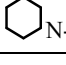
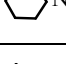
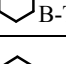
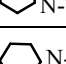
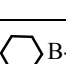
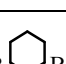
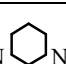
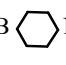

No. System	NICS(1Å)	NICS _{zz} (1Å)	Coupler HOMA values
1. IN-B  B-IN	-2.93	-4.41	0.957
2. IN-N  N-IN	-2.61	-2.67	0.901
3. IN-B  N-IN	-2.85	-3.56	0.921
4. IN-B  B-TTF	-2.78	-3.82	0.946
5. IN-N  N-TTF	-2.69	-2.34	0.869
6. IN-B  N-TTF	-2.49	-2.23	0.873
7. IN-N  B-TTF	-2.64	-3.47	0.926
8. TTF-B  B-TTF	-2.50	-3.60	0.939
9. TTF-N  N-TTF	-2.74	-2.81	0.872
10. TTF-B  N-TTF	-2.59	-3.01	0.907
Benzene	-11.12	-29.33	0.998
Borazine	-3.01	-5.93	0.942

^aThe NICS values are expressed in ppm units.

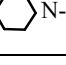
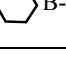
^bTo calculate HOMA we take $\alpha = 72.03 \text{ \AA}^{-2}$ and $R_0 = 1.402 \text{ \AA}$ for the B-N bond from the literature (see ref. [39(a-b)]). In the last row of this table we furnish HOMA values of free borazine and benzene at the same level of theory (for benzene see ref. [39]).

Table 2. Total energies (E , au) at optimized geometries using UB3LYP (part-I) and UM06 (part-II) levels of theory, $\langle S^2 \rangle$, intramolecular exchange-coupling constants (J , cm^{-1}) using the 6-311G(d,p) basis sets where Borazine and Benzene^a play the role of a coupler.

PART-I.

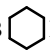
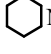
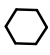
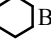

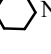
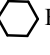
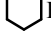
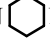
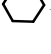
No.	System	Spin State	UB3LYP/6-311G(d,p) level of theory			
			$E(\text{a.u.})$	$\langle S^2 \rangle$	$J(\text{cm}^{-1})$ (Borazine)	$J(\text{cm}^{-1})$ (Benzene)
1.	IN-B  B-IN	Triplet	-1159.08754	2.04	41.70	26.24
		BS	-1159.08735	1.04		
2.	IN-N  N-IN	Triplet	-1159.02976	2.03	21.94	
		BS	-1159.02966	1.02		
3.	IN-B  N-IN	Triplet	-1159.05885	2.03	-59.26	-42.16
		BS	-1159.05912	1.03		
4.	IN-B  B-TTF	Triplet	-2523.40512	2.02	-2.13	-20.16
		BS	-2523.40513	0.99		
5.	IN-N  N-TTF	Triplet	-2523.34123	2.02	-34.77	
		BS	-2523.34139	1.01		
6.	IN-B  N-TTF	Triplet	-2523.37402	2.02	8.78	32.18
		BS	-2523.37398	1.02		
7.	IN-N  B-TTF	Triplet	-2523.37261	2.02	-132.89	
		BS	-2523.37327	0.93		
8.	TTF-B  B-TTF	Triplet	-3887.65572	2.01	2.20	0.92
		BS	-3887.65571	1.01		
9.	TTF-N  N-TTF	Triplet	-3887.58602	2.01	0.00	
		BS	-3887.58602	1.01		
10.	TTF-B  N-TTF	Triplet	-3887.62524	2.01	-2.20	-8.76
		BS	-3887.62525	1.01		

PART-II.

System	Spin State	UM06/6-311G(d,p) level of theory		
		$E(\text{a.u.})$	$\langle S^2 \rangle$	$J(\text{cm}^{-1})$
IN-B  N-TTF	Triplet	-2522.59516	2.02	2.19
	BS	-2522.59515	1.02	
IN-N  B-TTF	Triplet	-2522.59457	2.01	-12.78
	BS	-2522.59463	0.98	

^aThe E (au) and $\langle S^2 \rangle$ values of the benzene bridged diradicals are given in the supporting information.

Table 3. Correlation between the parity in terms of number of bonds along a spin-propagation path and the sign for the exchange coupling constant.

Diradical	Number of bonds in spin propagation path ^{a)}	Diradical	Number of bonds in spin propagation path ^{a)}
IN-B  B-IN	6 (J = 41.40)	IN-N  N-IN	6 (J = 21.94)
IN-B  N-IN	7 (J = -59.26)	IN-B  B-TTF	5 (J = -2.13)
IN-N  N-TTF	5 (J = -34.77)	IN-B  N-TTF	6 (J = 8.78)
IN-N  B-TTF	6 (J = -132.89)	TTF-B  B-TTF	4 (J = 2.20)
TTF-N  N-TTF	4 (J = 0.00)	TTF-B  N-TTF	5 (J = -2.20)

^{a)}J values are listed in parentheses, cm⁻¹.

Table 4. The energies of SOMOs and LUMO in *atomic units*, and their respective differences in eV, at the UB3LYP level of theory using a 6-311G(d,p) basis set.

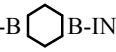
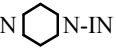
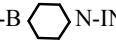
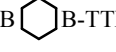
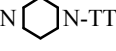
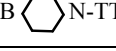
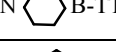
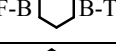
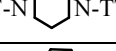
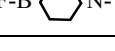
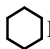
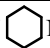
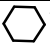
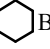
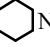
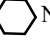
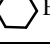
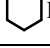
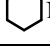
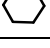
No.	Diradical	$E_{\text{HOMO-1}}$ (SOMO1)	E_{HOMO} (SOMO2)	E_{LUMO}	$\Delta E_{\text{SOMO-SOMO}}$	$\Delta E_{\text{HOMO-LUMO}}$
1.	IN-B  B-IN	-0.20901	-0.20855	-0.04634	0.013	4.414
2.	IN-N  N-IN	-0.20887	-0.20821	-0.01483	0.018	5.262
3.	IN-B  N-IN	-0.21443	-0.20620	-0.04867	0.224	4.287
4.	IN-B  B-TTF	-0.33060	-0.28257	-0.18636	1.307	2.618
5.	IN-N  N-TTF	-0.32269	-0.28615	-0.18345	0.994	2.795
6.	IN-B  N-TTF	-0.32566	-0.28681	-0.18629	1.057	2.735
7.	IN-N  B-TTF	-0.33232	-0.27487	-0.18964	1.563	2.319
8.	TTF-B  B-TTF	-0.39294	-0.39294	-0.24990	0.000	3.892
9.	TTF-N  N-TTF	-0.39196	-0.38440	-0.25222	0.206	3.597
10.	TTF-B  N-TTF	-0.39162	-0.39098	-0.25337	0.017	3.745


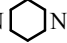
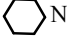
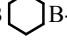
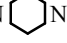
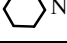
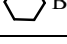
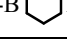
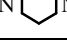
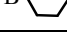
Table 5. The relationship between the structural symmetry of diradicals (monoradical-combinations^{a)} and connector-atoms^{b)} with energy differences $\Delta E_{\text{SOMO-SOMO}} = E(\text{SOMO2}) - E(\text{SOMO1})$, in eV, at the UB3LYP level of theory using a 6-311G(d,p) basis set.

No.	Diradical	<i>Mono-radical-combination/Connector-Atoms</i>	$\Delta E_{\text{SOMO-SOMO}}$
	IN-B  B-IN	SYM / SYM	0.013
	IN-N  N-IN	SYM / SYM	0.018
	IN-B  N-IN	SYM / NONSYM	0.224
	IN-B  B-TTF	NONSYM / SYM	1.307
	IN-N  N-TTF	NONSYM / SYM	0.994
	IN-B  N-TTF	NONSYM / NONSYM	1.057
	IN-N  B-TTF	NONSYM / NONSYM	1.563
	TTF-B  B-TTF	SYM / SYM	0.000
	TTF-N  N-TTF	SYM / SYM	0.206
	TTF-B  N-TTF	SYM / NONSYM	0.017

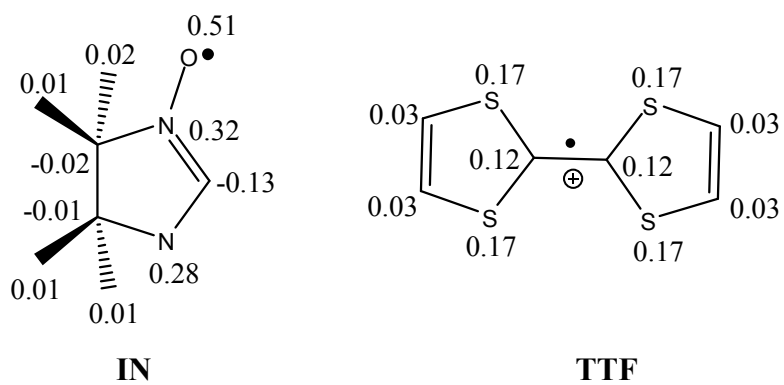
^{a)} The symmetric monoradical combinations are: (IN,IN), (TTF,TTF);
Non-symmetric monodiradical combination is (IN,TTF).

^{b)} The symmetric connector-atom combinations are: (B,B), (N,N);
Non-symmetric connector-atom combination is (B,N).

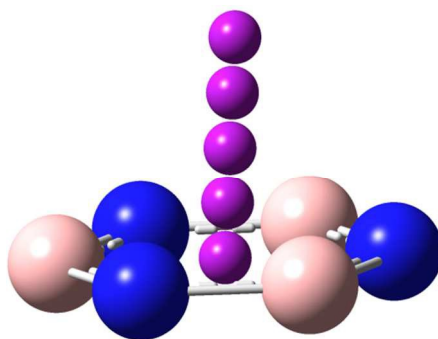
Table 6. Natural orbital occupations of these diradicals in their triplet state using the UB3LYP/6-311G(d,p) level of theory.

No.	Diradicals	HOMO-2	HOMO-1 (SOMO1)	HOMO (SOMO2)	LUMO
1.	IN-B  B-IN	1.992	1.0	1.0	0.008
2.	IN-N  N-IN	1.992	1.0	1.0	0.008
3.	IN-B  N-IN	1.995	1.0	1.0	0.005
4.	IN-B  B-TTF	1.992	1.0	1.0	0.008
5.	IN-N  N-TTF	1.991	1.0	1.0	0.009
6.	IN-B  N-TTF	1.995	1.0	1.0	0.005
7.	IN-N  B-TTF	1.995	1.0	1.0	0.005
8.	TTF-B  B-TTF	2.000	1.0	1.0	0.000
9.	TTF-N  N-TTF	1.999	1.0	1.0	0.001
10.	TTF-B  N-TTF	1.999	1.0	1.0	0.001

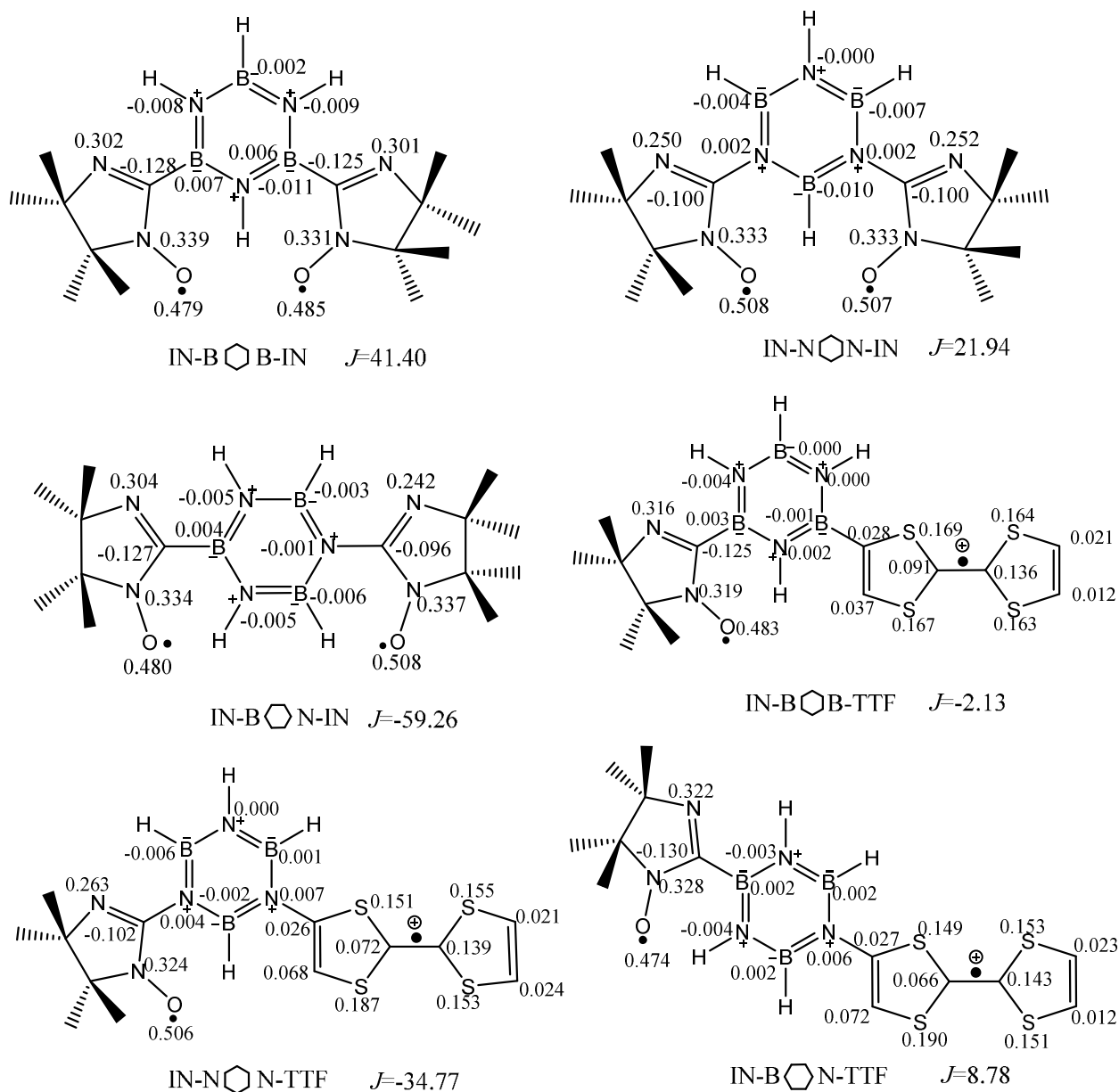
Scheme 1: The schematic representation of the structures of imino-nitroxide (IN) and tetrathiafulvalene-cation (TTF) radical moieties with atomic spin-populations in their ground state using B3LYP/6-311G(d,p) level of theory.

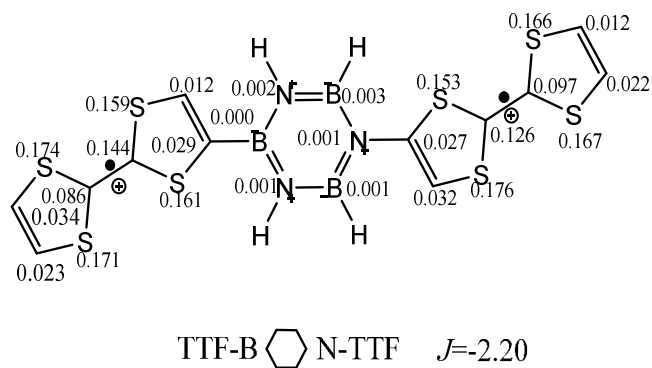
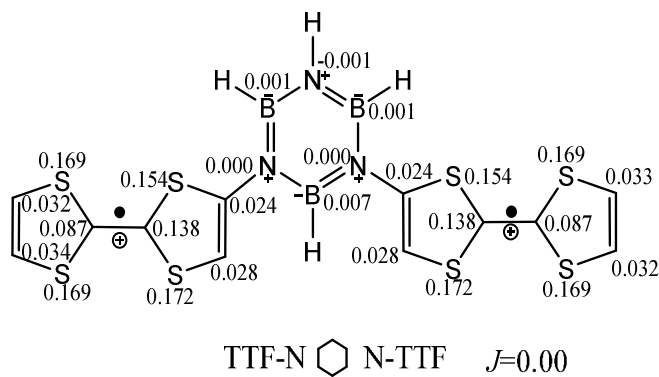
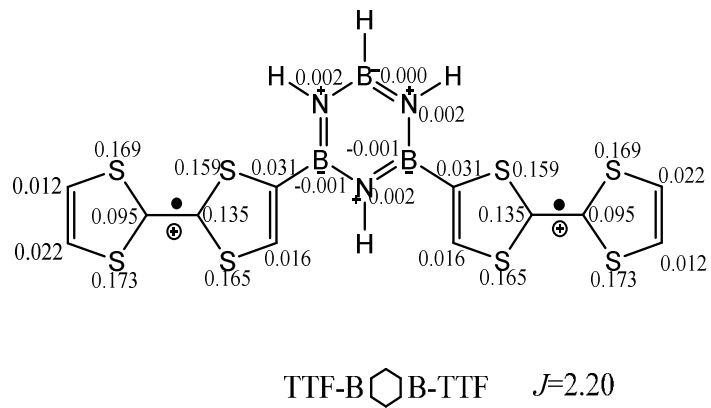
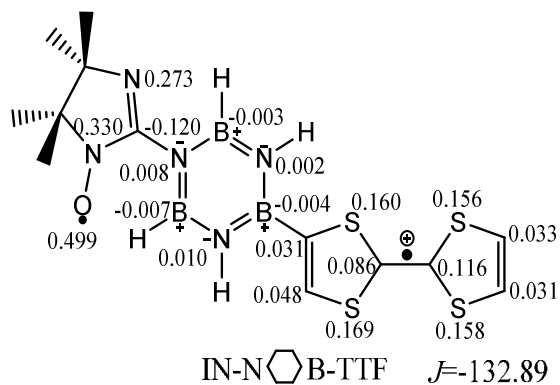


Scheme 2. The probe atom is placed at regular intervals of 0.5\AA from the π -surface of the borazine-ring coupler of these diradicals. The blue, pink and magenta colours represent the nitrogen, boron and probe atom, respectively. The hydrogen atoms are omitted for clarity.

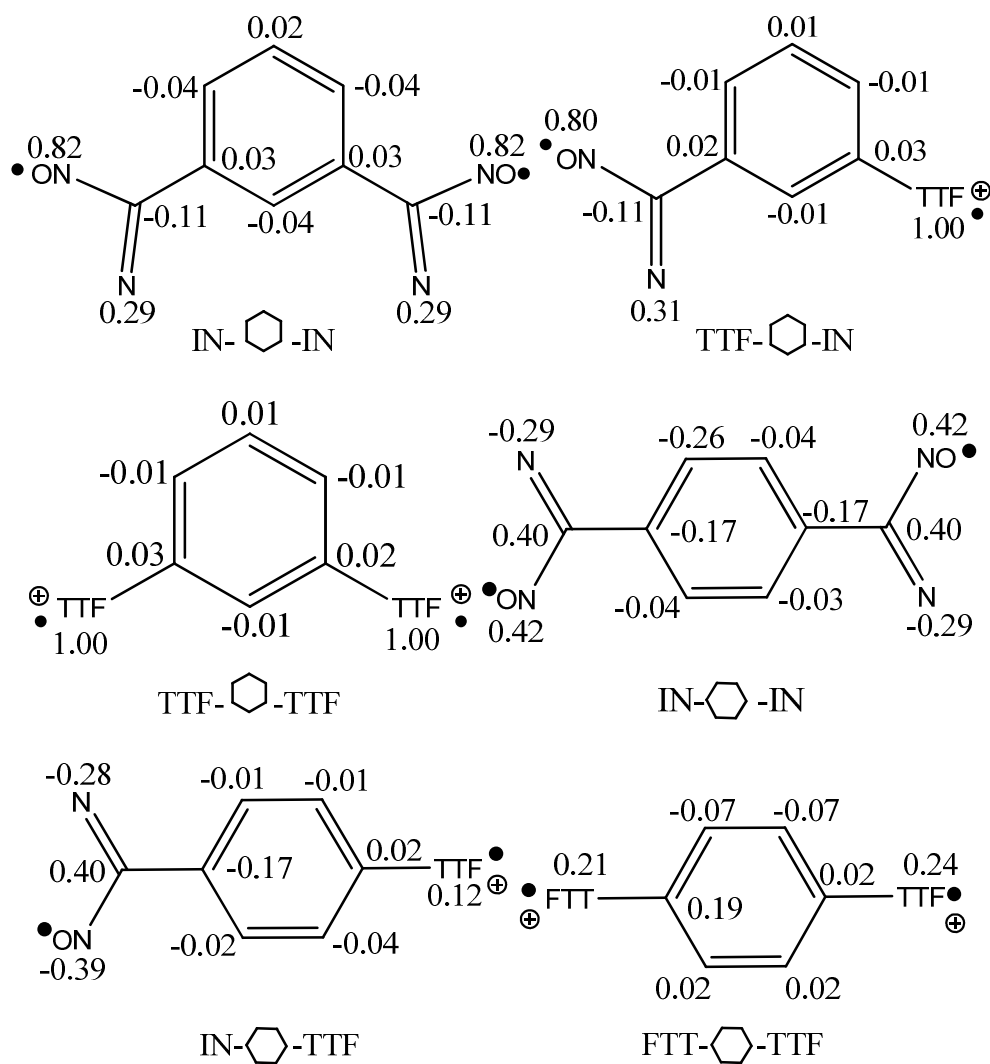


Scheme 3: The schematic representation of different linkage specific borazine coupled (*meta*-B-B, *meta*-N-N and *para*-B-N connected) diradicals investigated showing their atomic spin-populations in their triplet states up to three decimal places.





Scheme 4: Schematic representation of the atomic spin-populations for the corresponding benzene-coupled diradicals with the same radical moieties taken for our borazine coupler.



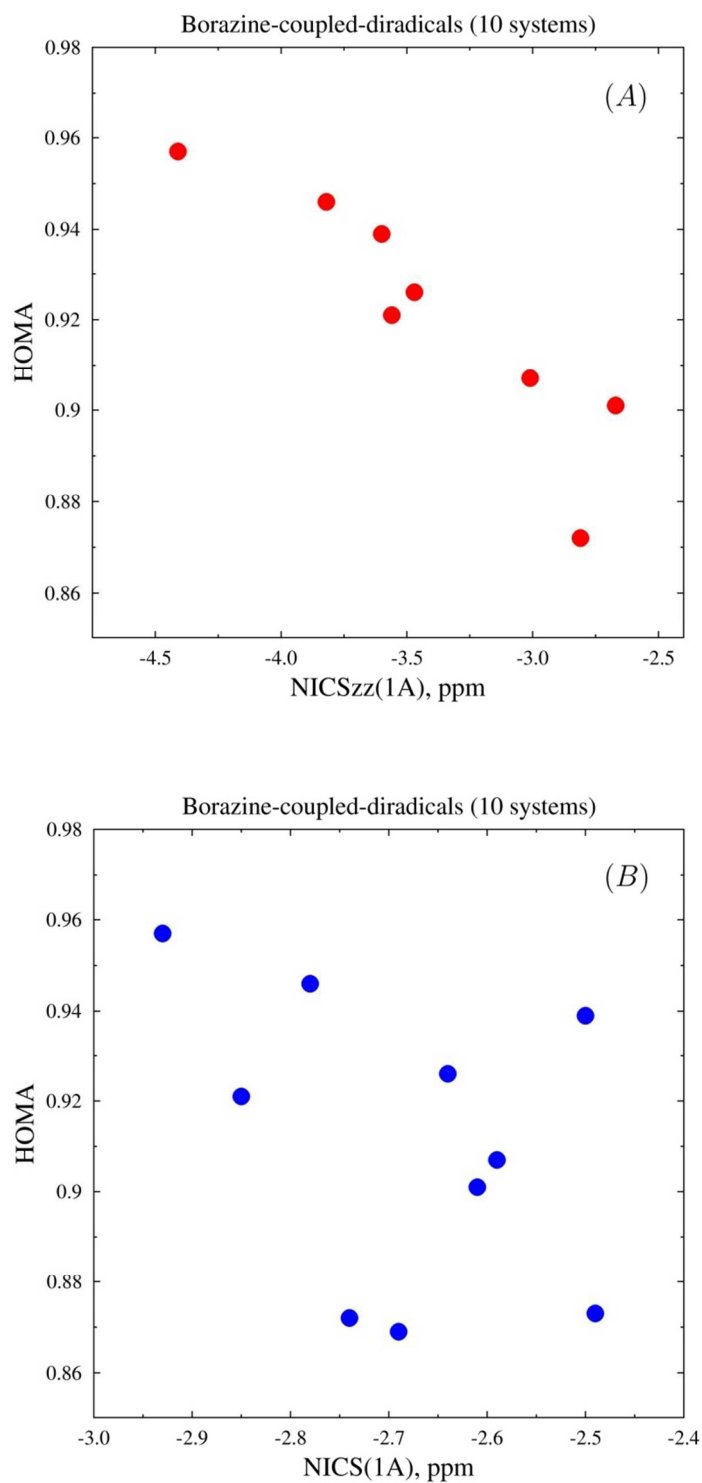


Figure 1. Panel (A): Plot of HOMA versus NICSzz(1Å).
Panel (B): Plot of HOMA versus NICS(1Å).

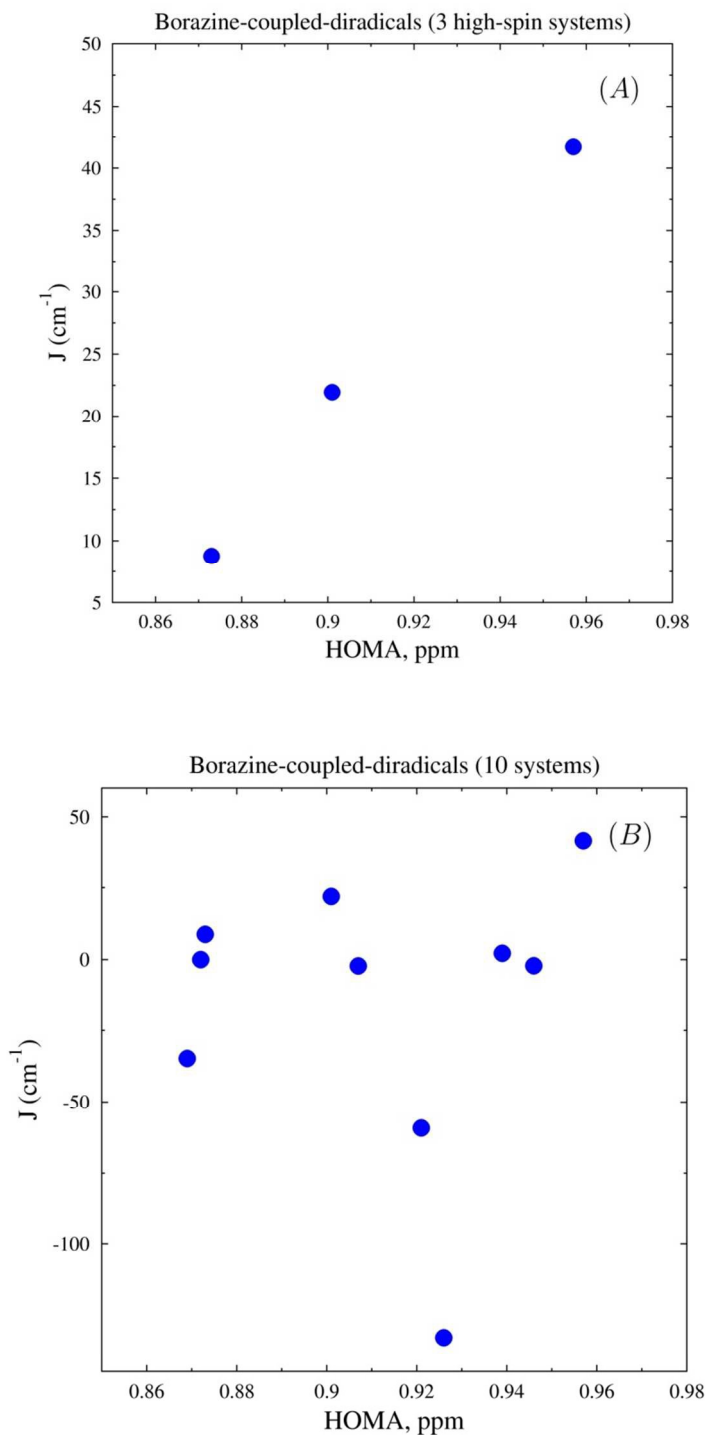


Figure 2. Plot of exchange-coupling constants J (cm^{-1}) versus HOMA aromaticity indices. Panel (A): Only high-spin borazine-coupled diradical species ($J > 5 \text{ cm}^{-1}$). Panel (B): Complete set of 10 borazine-coupled diradical systems.

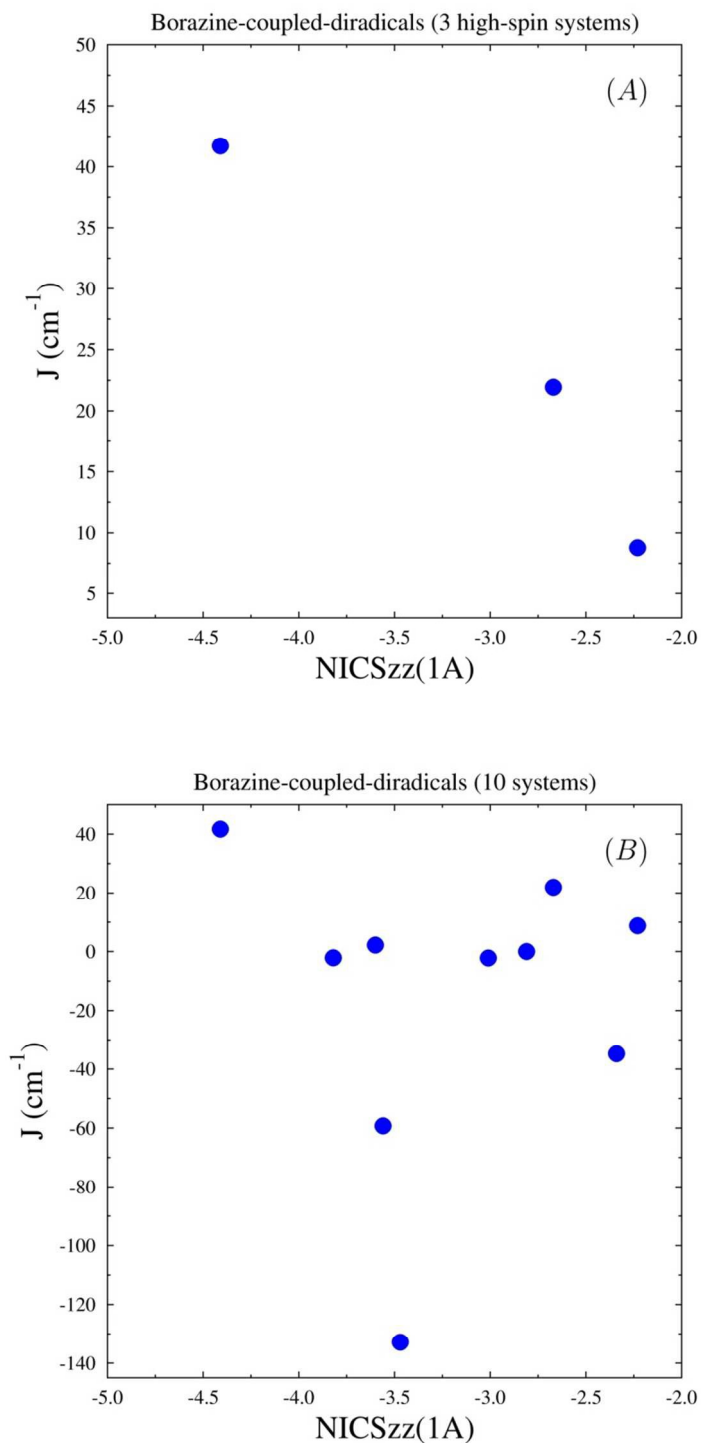


Figure 3. Plot of exchange-coupling constants J (cm^{-1}) versus NICSzz(1Å) indices. Panel (A): Only high-spin borazine-coupled diradical species ($J > 5 \text{ cm}^{-1}$). Panel (B): Complete set of 10 borazine-coupled diradical systems.

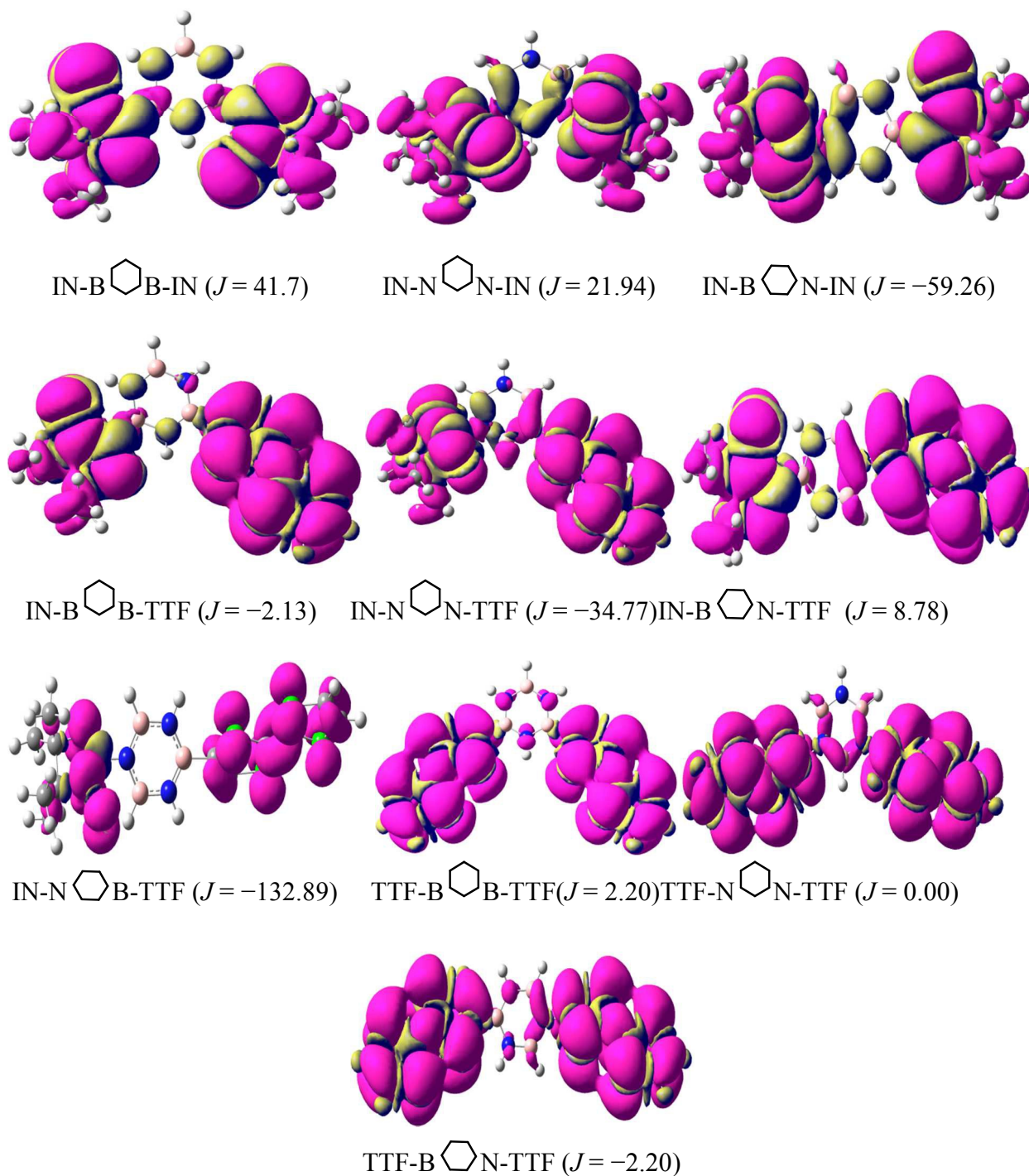


Figure 4: The spin-density distribution plots of the studied diradicals at the UB3LYP/6-311G(d,p) level of theory in their triplet states. The mauve and yellow colors respectively represent the up-spin and down-spin density. The iso-value taken for these figures is 0.001.

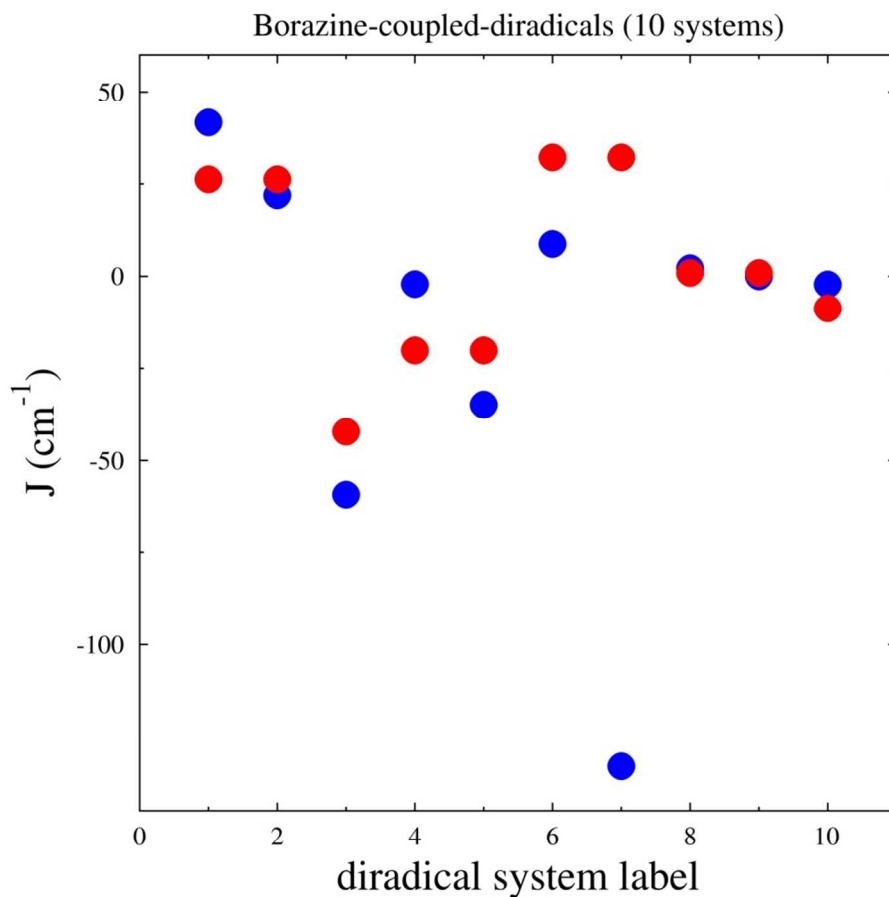


Figure 5. The comparison of J values between Borazine-coupled diradicals (Blue symbols) and Benzene-coupled diradicals (Red symbols) for all 10 systems. The ordering of systems follows the convention in **Table 1**. The high-spin diradical states correspond to cases where $J > 0 \text{ cm}^{-1}$ and low-spin diradicals are represented by $J < 0 \text{ cm}^{-1}$ values. Finally, the diradical states with $J = 0 \text{ cm}^{-1}$ values correspond to diamagnetic (non-magnetic) states.

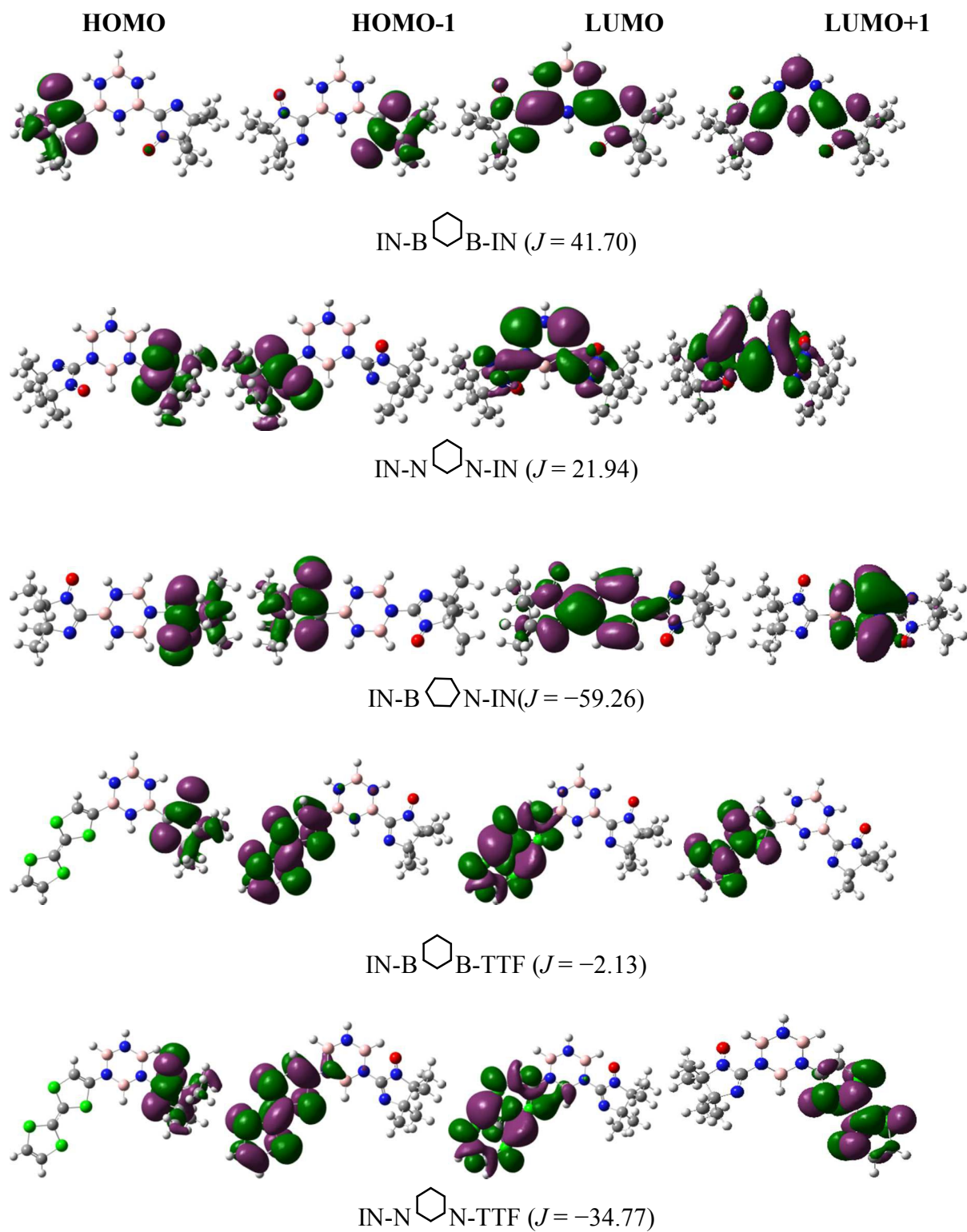


Figure 6. Spatial distribution of the HOMO, HOMO-1, LUMO and LUMO-1 of different diradicals at the UB3LYP/6-311G(d,p) level of theory in their triplet states.

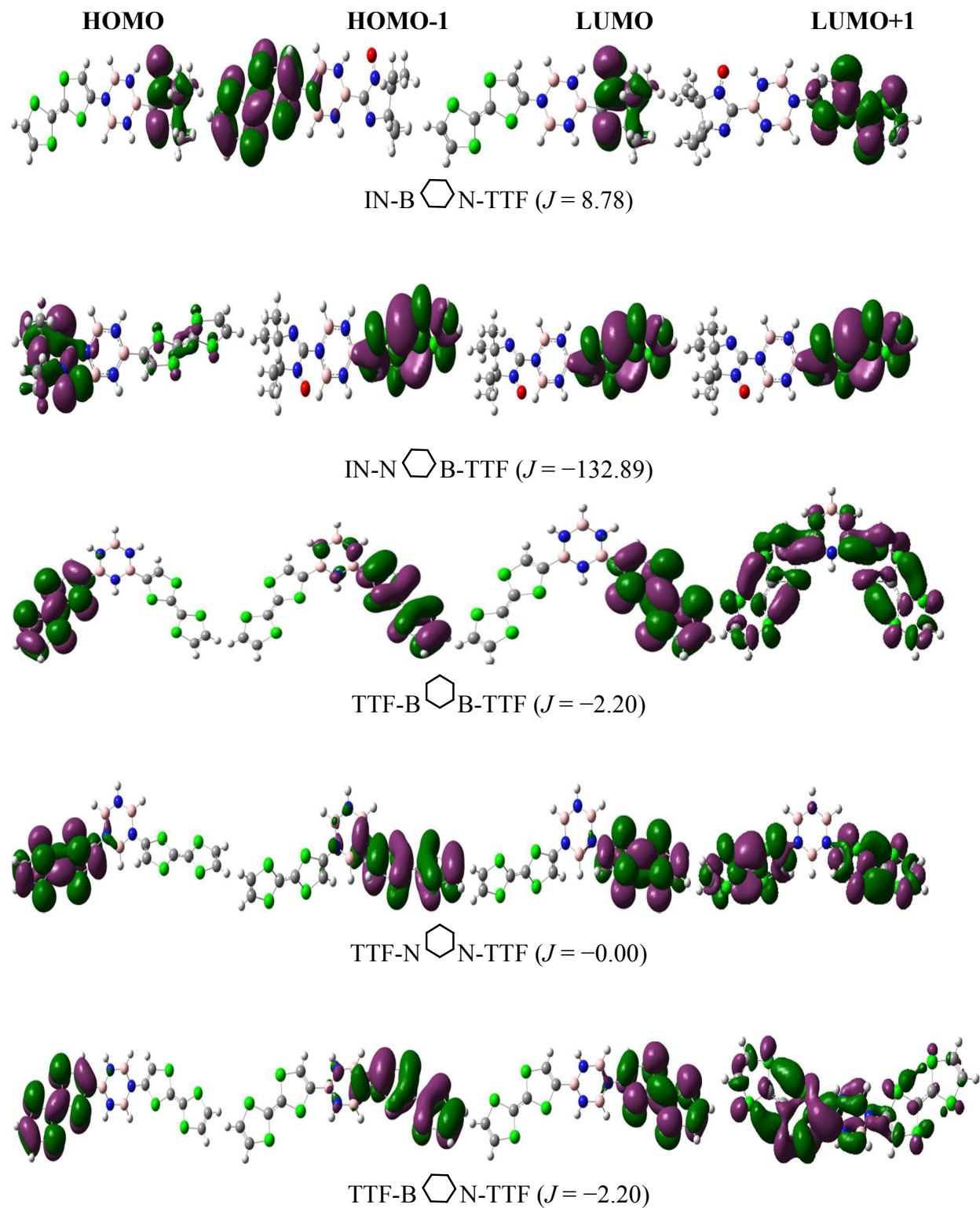


Figure 6 (continue). Spatial distribution of the HOMO, HOMO-1, LUMO and LUMO-1 of different diradicals at the UB3LYP/6-311G(d,p) level of theory in their triplet states.

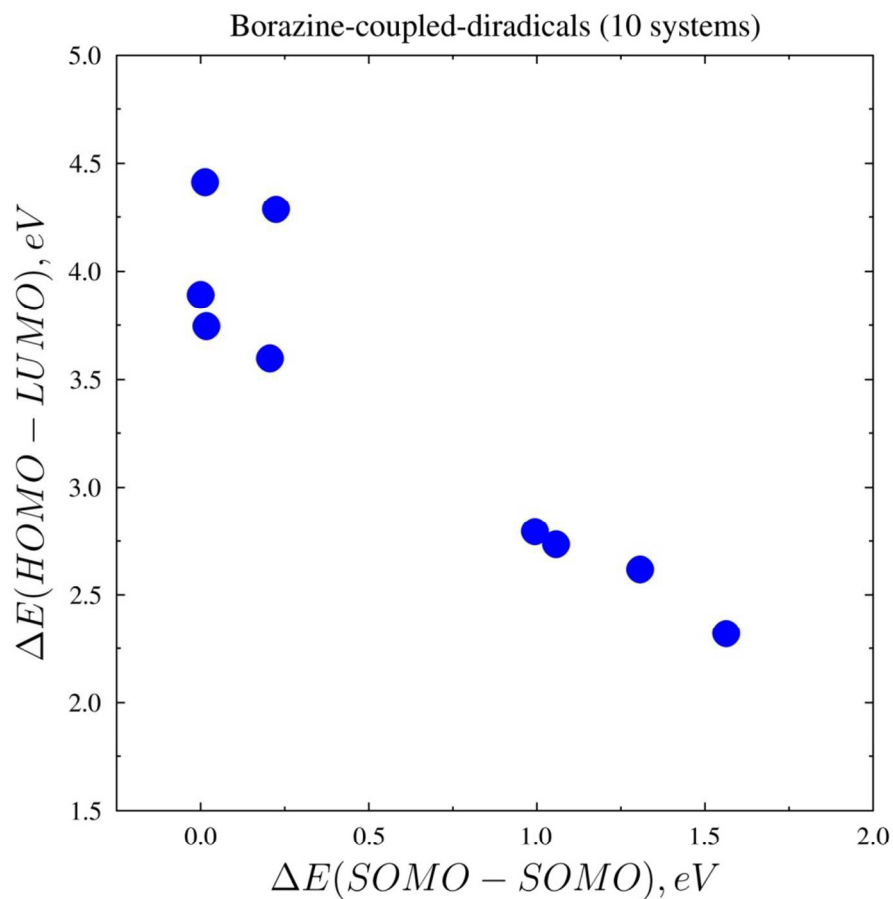
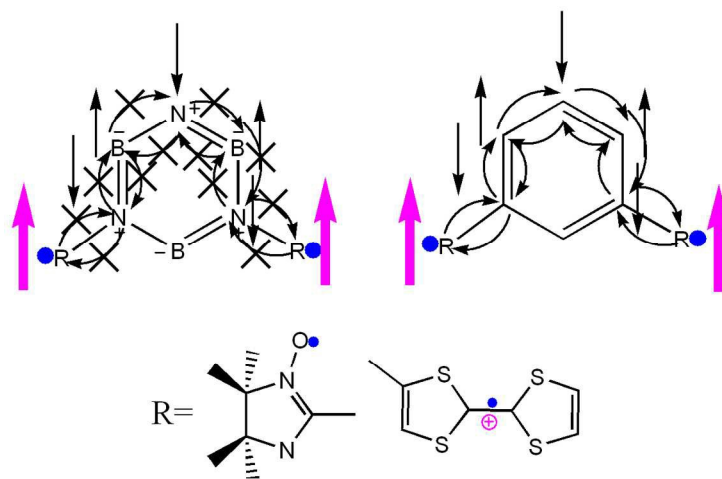


Figure 7. Plot of $\Delta E(HOMO-LUMO)$ values versus $\Delta E(SOMO-SOMO)$ values for all 10 borazine-coupled diradical species.

Table of Content (TOC) Graphics



Spin-blocker capacity of borazine is investigated for *meta*-BB, *meta*-NN and *para*-BN structures highlighting the correlation between magnetic properties and aromaticity.